

Flexible photovoltaic cells based on a graphene–CdSe quantum dot nanocomposite†

Jing Chen,^a Feng Xu,^a Jun Wu,^a Khan Qasim,^a Yidan Zhou,^a Wei Lei,^{*a} Li-Tao Sun^a and Yan Zhang^b

Received 4th November 2011, Accepted 21st November 2011

DOI: 10.1039/c2nr11656a

We have fabricated the flexible photoelectrode by loading graphene sheets modified with CdSe QDs. A power conversion efficiency of ~0.6% and an incident photon to current conversion efficiency of 17% have been achieved for this flexible photovoltaic cell based on a graphene–CdSe nanocomposite.

Quantum dot sensitized solar cells (QDSSCs) have attracted extensive interest as a means of fabricating highly efficient, low cost photovoltaics.¹ In the QDSSC, quantum dots (QDs), such as CdS,² CdSe,³ and CdTe,⁴ are attached to a wide band gap semiconductor, usually TiO₂⁵ or ZnO^{6,7} as the photoanode. Following light absorption, the electrons are injected while the holes are transported *via* a suitable electrolyte to the counter-electrode.⁶ Due to the impact ionization effect, it is possible to utilize hot electrons in QDs to generate multiple electron–hole pairs per photon.⁸ Thus, the power conversion efficiency of QDSSCs is expected to exceed the Shockley and Queisser limit of 31%.⁹

Despite these features, the efficiencies of QDSSCs based on these conventional photoanodes are rather low. Efficient electron–hole pair disassociation and electron collection are still big challenges for QDSSCs. Various strategies have been employed to reduce the carrier recombination.^{10,11} One way to improve charge separation is to develop novel composite nanostructures. Kamat and Brown have reported a CdSe–C₆₀ composite employed in the QDSSC and C₆₀ played an effective role to capture and transfer photogenerated electrons to the surface of the electrode.¹² In addition, they reported the use of a CdS–CNT structure as the light-harvesting assembly and obtained ~1% of incident photon-to-charge carrier generation efficiency.¹³ Compared with CNT, graphene is more efficient for application in photovoltaic cells due to its unique structural mechanical, chemical and electronic properties.¹⁴ The high carrier mobility of graphene can facilitate electron transport to the photoanode, thereby

decreasing the probability for carrier recombination and extending its lifetime.¹⁵ In addition, the giant surface area of graphene makes it highly desirable as a supporting material.¹⁶ Modification of the graphene surface with QDs causes the fluorescence quenching due to the electrons flow from the conduction band of the QD to the graphene sheets.¹⁷ Therefore, the hybrid nanostructures based on graphene can be considered as the potential building blocks for photoelectrochemical cells. For example, Guo *et al.* have reported the layered graphene/CdS architecture employed in QDSSCs and an external quantum yield of 16% was achieved.¹⁸ In this article, we shall present a facile method for assembling graphene–CdSe (G–CdSe) nanocomposites (NPs) on the flexible substrate by electrophoretic deposition. The power conversion efficiency (PCE) of ~0.6% for this variety of the flexible QDSSC is also obtained.

The procedure for fabrication of G–CdSe NPs and QDSSCs is described in the ESI†. Fig. 1(a) shows the absorption spectra of solutions for CdSe QD, graphene and G–CdSe, respectively. From the excitonic transition peaks at 563 nm for the CdSe QD solution, the size of the QDs is estimated to be 3.3 nm, based on the analysis reported in the literature.¹⁹ Compared with the pure CdSe QD, the G–CdSe NP maintains the excitonic peak without any obvious

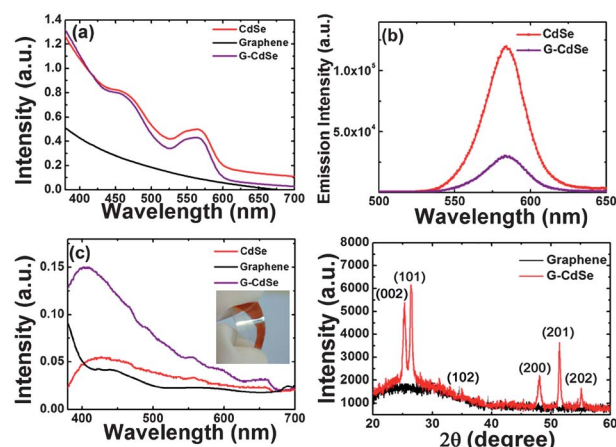


Fig. 1 (a) Absorption spectra of solutions for CdSe QD, graphene, and G–CdSe; (b) PL spectra of solutions for CdSe QDs and G–CdSe; (c) absorption spectra of photoanodes based on CdSe QD, graphene and G–CdSe, the inset shows the flexible photoanode of a G–CdSe film; (d) XRD spectra of graphene and G–CdSe.

^aSchool of Electronic Science and Engineering, Southeast University, Nanjing, 210096, China. E-mail: lw@seu.edu.cn; Fax: +86 25 83792662; Tel: +86 25 83792650

^bElectrical Engineering Division, Engineering Department, University of Cambridge, 9 JJ Thomson Avenue, CB3 0FA Cambridge, UK. E-mail: yz236@cam.ac.uk

† Electronic supplementary information (ESI) available: Experimental procedure, Raman spectra of graphene, CdSe QD and G–CdSe film, AFM images of graphene, PDDA modified graphene and G–CdSe film, electron transfer rate constant analysis for films based on 2.7 nm, 3.3 nm and 4.1 nm CdSe QDs. See DOI: 10.1039/c2nr11656a

change, which indicates that almost no QD agglomeration has taken place on the G-CdSe film. Fig. 1(b) shows the photoluminescence (PL) spectra of pure CdSe and G-CdSe NP solution. From the analysis it is depicted that the characteristic emission peak of the CdSe QD is located at 580 nm and about 75% of CdSe QD emission is quenched after CdSe QDs interacted with graphene sheets. It has been demonstrated that the graphene sheets are expected as the electron acceptor, which favor the electron transfer pathway.

Fig. 1(c) shows the absorption spectra of photoanodes of graphene, CdSe QD and G-CdSe NP. There seems to be no prominent peak in the visible region for the pure graphene photoanode. Compared to the pure CdSe QD photoanode, the absorption intensity is greatly enhanced for the G-CdSe NP photoanode. The inset of Fig. 1(c) shows the photoimage of the flexible electrode of a G-CdSe NP. The G-CdSe NP is uniformly and firmly loaded on the flexible substrate. Fig. 1(d) shows the X-ray diffraction spectra (XRD) of graphene and G-CdSe NP. The main diffraction peaks of (002), (101) and (102) crystal planes can be detected, which correspond to the values of the wurtzite structure (JCPDS no.02-0330).

Fig. 2(a) and (b) show the transmission electron microscopy (TEM) images of graphene and CdSe QDs. Graphene possesses a clear and smooth surface with mono- and multi-layered sheets. CdSe QDs with a diameter of 3–4 nm uniformly disperse in the ethanol solution, which is in good agreement with the absorption results.

Fig. 2(c) and (d) show the TEM and high-resolution transmission electron microscopy (HRTEM) images of a G-CdSe NP. It can be seen that the QDs are uniformly and densely assembled on the surface of graphene sheets. The exchange of the ligand capped CdSe from oleic acid (OA) to mercaptopropionic acid (MPA) resulted in an increased affinity with the hydrophobic carbon surface. Consequently, the QDs self-assembled on the surface of graphene *via* electrostatic interactions between the negatively charged MPA modified CdSe QDs and positively charged graphene, which was noncovalently functionalized with poly(diallyldimethylammonium chloride) (PDDA).²⁰ From Fig. 2(d), it is demonstrated that the CdSe QD has good crystallization with lattice spacing *ca.* 0.352 nm for the (002) plane of CdSe, which is consistent with the XRD results.

Fig. 3(a) and (b) show the cross-sectional and top-view scanning electron microscopy (SEM) images of the photoanode based on a

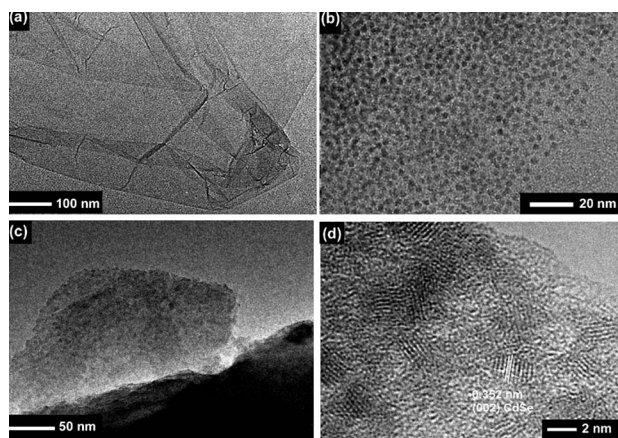


Fig. 2 TEM images of (a) graphene sheets; (b) CdSe QDs; (c) G-CdSe NP; and (d) HRTEM image of a G-CdSe NP.

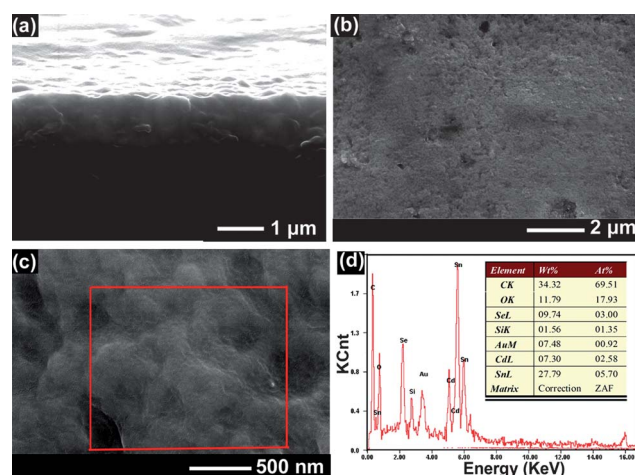


Fig. 3 (a) Cross-sectional and (b) top-view SEM images of a G-CdSe film on the PET/ITO substrate; (c) magnified SEM image of the G-CdSe film; (d) EDX spectra of the G-CdSe film.

G-CdSe NP. It is seen that the film composed of a G-CdSe NP is closely packed on the substrate with a uniform thickness of $\sim 1 \mu\text{m}$. Fig. 3(c) shows the magnified SEM image and the energy dispersive X-ray (EDX) spectroscopy of G-CdSe photoanode is presented in Fig. 3(d). From the analysis, the ratio of Cd : Se is close to 1 : 1. The Sn originates from the substrate, which forms the SnO_2 layer. And the high concentration of C is not only from graphene, but also from the ligand capped CdSe QDs.

The energy level schematic diagram of the QDSSC consisting of SnO_2 , graphene, CdSe QD and ZnS coating layer is shown in Fig. 4 (a). From the excitonic transition wavelength of 563 nm for the CdSe QDs [Fig. 1(a)], the band gap of the QD is estimated to be around 2.21 eV. The work function of a typical graphene is 4.4–4.5 eV.²¹ Therefore, this energetic arrangement favors the photogenerated electrons transfer from excited CdSe to graphene.

To investigate the performance variation of QDSSCs based on different sizes of CdSe QD modified graphene, we fabricated

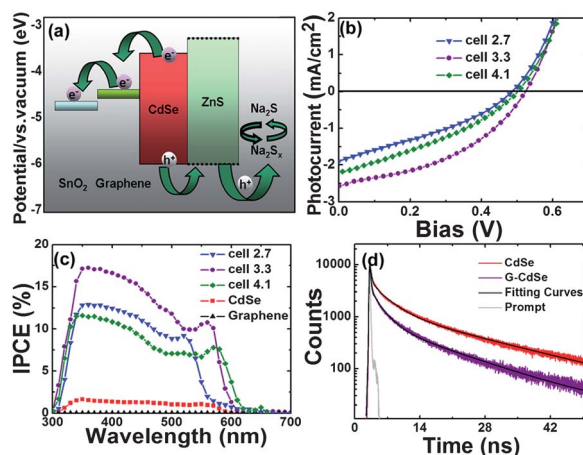


Fig. 4 (a) Energy level schematic diagram of the QDSSC; (b) *I*-*V* characteristics of three cells; (c) IPCE spectra for QDSSCs based on graphene, CdSe and G-CdSe (three cells); (d) the emission decay profiles for CdSe QDs and G-CdSe.

Table 1 Photovoltaic parameters for cell 2.7, cell 3.3 and cell 4.1 and QDSSCs based on bare graphene and bare CdSe QD

	$J_{sc}/\text{mA cm}^{-2}$	V_{oc}/V	FF	PCE
Cell 2.7	1.91	0.49	31.5%	0.34%
Cell 3.3	2.56	0.52	41.8%	0.58%
Cell 4.1	2.14	0.50	34.0%	0.38%
Graphene	0.02	0.28	34.6%	0.02%
CdSe QD	0.30	0.58	39.8%	0.06%

QDSSCs based on 2.7 nm, 3.3 nm and 4.1 nm CdSe QD modified graphene, respectively, named as cell 2.7, cell 3.3 and cell 4.1. Fig. 4(b) shows the current–voltage (I – V) characteristics of the three cells with Na_2S electrolyte under a simulated AM 1.5 G solar irradiation with a light intensity of 100 mW cm^{-2} . In addition, QDSSCs based on pure graphene and pure CdSe QDs were also prepared in this study, whose related photovoltaic parameters are listed in Table 1. In the table, it is seen that the short-circuit current density (J_{sc}) value is very small for QDSSCs fabricated on the pure CdSe film. The performance dramatically increased for cell 2.7, cell 3.3 and cell 4.1, with maximum enhancement achieved for the 3.3 nm CdSe QD photoelectrode (cell 3.3). The J_{sc} of cell 3.3 is largely enhanced by about 7-fold compared to that of the QDSSC based on the pure CdSe film. This confirms that the graphene sheet can be used as a good conducting scaffold to capture and transport electrons in the photoanode. The maximum PCE value of cell 3.3 is 0.58% with $J_{sc} = 2.56 \text{ mA cm}^{-2}$ and $V_{oc} = 0.52 \text{ V}$, which is higher than cell 2.7 (0.34%) and cell 4.1 (0.38%). It is worth mentioning that the performance of QDSSCs can be increased greatly after coating with ZnS as the passivation layer, which can reduce the undesired surface trapping processes.²² Meanwhile, it is reported that the ZnS layer also increases the rate of electron transfer.²³ Therefore, the charge recombination can be decreased and photocurrent can be increased, thereby leading to an improved performance in QDSSCs.

The incident photon to current conversion efficiency (IPCE) was measured for graphene, CdSe and G–CdSe devices [Fig. 4(c)] in the range of 300 to 700 nm. The IPCE value for graphene is very small, which is in agreement with the output I – V characteristics. To our knowledge, there is no report on the QDSSC based on pure graphene photoanode and the mechanism of photocurrent generated by graphene is not very clear. In our further work, we shall study and reveal the mechanism of graphene employed in the QDSSC. The IPCE values for cell 2.7, cell 3.3 and cell 4.1 at 350 nm are 11%, 17% and 13%, respectively, which show more than a 8 to 10 fold enhancement over that of the QDSSC based on pure CdSe (2.4%). Thus, the higher J_{sc} value for a QDSSC based on a G–CdSe NP can be achieved for cell 3.3 due to its higher photon-to-electron conversion capability in the presence of graphene sheets. From Fig. 4(c), it is seen that the onset increased to longer wavelengths for the larger sizes of CdSe QDs, in correspondence with a broader light harvest range of the QDs. Conversely, the photocurrent is generated in a narrower range for the cell using smaller sized QDs, leading to a lower value of J_{sc} and PCE. Therefore, cell 2.7 has a lower PCE value than that of cell 3.3.

In order to further understand the increase in the device performance, the emission decays of cell 2.7, cell 3.3 and cell 4.1 were measured. Fig. 4(d) shows the emission decay profiles for CdSe QDs and G–CdSe with 3.3 nm CdSe QDs, supporting the quenching of

the CdSe QDs by graphene sheets. The multiexponential decay shows that the average emission lifetimes of CdSe with and without graphene sheets are 4.4 ns and 1.6 ns, respectively. Thus, an average electron transfer rate constant of $3.6 \times 10^8 \text{ s}^{-1}$ can be calculated as shown in Table S1† (ESI)†. These results indicate that it is an effective approach to collect and transport photogenerated electrons from CdSe in the presence of graphene. In light of the previous report,²⁴ the electron transfer rate was found to decrease exponentially with increasing size of CdSe QDs. Herein, we found a similar trend of the electron transfer rate from CdSe QD to graphene reducing with increasing sizes of CdSe QDs as shown in Fig. S3† (ESI)†. Therefore, the energetic driving force for electron transfer from CdSe to graphene can be reduced due to the downward shift of the CdSe conduction level with increasing QD size, leading to a lower PCE value for cell 4.1 as compared to cell 3.3.

In summary, the deposition of CdSe on graphene sheets has been successfully achieved in suspensions as well as in films. The PCE of the QDSSC was $\sim 0.6\%$ and a corresponding IPCE up to 17% was obtained. The electron-transfer rate was calculated to be $3.6 \times 10^8 \text{ s}^{-1}$ with an average lifetime of 1.7 ns for 3.3 nm CdSe QDs on graphene sheets. Therefore, compared to pure graphene and pure CdSe QDs, the enhanced performance can be obtained for the flexible QDSSC based on a G–CdSe film confirming that the G–CdSe NP can be used as a potential architecture employed in photovoltaic cells.

Notes and references

- 1 D. R. Baker and P. V. Kamat, *Adv. Funct. Mater.*, 2009, **19**, 805–811.
- 2 C. H. Chang and Y. L. Lee, *Appl. Phys. Lett.*, 2007, **91**, 053503.
- 3 J. Chen, J. L. Song, X. W. Sun, W. Q. Deng, C. Y. Jiang, W. Lei, J. H. Huang and R. S. Liu, *Appl. Phys. Lett.*, 2009, **94**, 153115.
- 4 X. F. Gao, H. B. Li, W. T. Sun, Q. Chen, F. Q. Tang and L. M. Peng, *J. Phys. Chem. C*, 2009, **113**, 7531–7535.
- 5 J. Chen, J. L. Song, X. W. Sun, W. Q. Deng, C. Y. Jiang, W. Lei, J. H. Huang and R. S. Liu, *Appl. Phys. Lett.*, 2009, **94**, 153115.
- 6 F. Xu and L. Sun, *Energy Environ. Sci.*, 2011, **4**, 818–841.
- 7 F. Xu, M. Dai, Y. Lu and L. Sun, *J. Phys. Chem. C*, 2010, **114**, 2776–2782.
- 8 A. J. Nozik, *Inorg. Chem.*, 2005, **44**, 6893–6899.
- 9 W. Shockley and H. J. Queisser, *J. Appl. Phys.*, 1961, **32**, 510.
- 10 I. Mora-Sero, S. Gimenez, F. Fabregat-Santiago, R. Gomez, Q. Shen, T. Toyoda and J. Bisquert, *Acc. Chem. Res.*, 2009, **42**, 1848–1857.
- 11 J. Chen, C. Li, D. W. Zhao, W. Lei, Y. Zhang, M. T. Cole, D. P. Chu, B. P. Wang, Y. P. Cui, X. W. Sun and W. I. Milne, *Electrochem. Commun.*, 2010, **12**, 1432–1435.
- 12 P. Brown and P. V. Kamat, *J. Am. Chem. Soc.*, 2008, **130**, 8890–8891.
- 13 I. Robel, B. A. Bunker and P. V. Kamat, *Adv. Mater.*, 2005, **17**, 2458.
- 14 S. Iijima, *Nature*, 1991, **354**, 56–58.
- 15 S. R. Sun, L. Gao and Y. Q. Liu, *Appl. Phys. Lett.*, 2010, **96**, 083113.
- 16 P. V. Kamat, *J. Phys. Chem. Lett.*, 2011, **1**, 520–527.
- 17 A. N. Cao, Z. Liu, S. S. Chu, M. H. Wu, Z. M. Ye, Z. W. Cai, Y. L. Chang, S. F. Wang, Q. H. Gong and Y. F. Liu, *Adv. Mater.*, 2010, **22**, 103.
- 18 C. X. Guo, H. B. Yang, Z. M. Sheng, Z. S. Lu, Q. L. Song and C. M. Li, *Angew. Chem., Int. Ed.*, 2010, **49**, 3014–3017.
- 19 W. W. Yu, L. H. Qu, W. Z. Guo and X. G. Peng, *Chem. Mater.*, 2003, **15**, 2854–2860.
- 20 L. L. Li, K. P. Liu, G. H. Yang, C. M. Wang, J. R. Zhang and J. J. Zhu, *Adv. Funct. Mater.*, 2011, **21**, 869–878.
- 21 R. Czerw, B. Foley, D. Tekleab, A. Rubio, P. M. Ajayan and D. L. Carroll, *Phys. Rev. B: Condens. Matter*, 2002, **66**, 033408.
- 22 A. Salant, M. Shalom, I. Hod, A. Faust, A. Zaban and U. Banin, *ACS Nano*, 2010, **4**, 5962–5968.
- 23 N. Guijarro, J. M. Campin, Q. Shen, T. Toyoda, T. Lana-Villarreal and R. Gomez, *Phys. Chem. Chem. Phys.*, 2011, **13**, 12024–12032.
- 24 A. Kongkanand, K. Tvrđy, K. Takechi, M. Kuno and P. V. Kamat, *J. Am. Chem. Soc.*, 2008, **130**, 4007–4015.